

## Order - disorder transition in $\text{Cu}_3\text{Au}$ : a density functional approach

This article has been downloaded from IOPscience. Please scroll down to see the full text article.

1997 J. Phys.: Condens. Matter 9 87

(<http://iopscience.iop.org/0953-8984/9/1/011>)

View [the table of contents for this issue](#), or go to the [journal homepage](#) for more

Download details:

IP Address: 171.66.16.207

The article was downloaded on 14/05/2010 at 06:02

Please note that [terms and conditions apply](#).

# Order–disorder transition in $\text{Cu}_3\text{Au}$ : a density functional approach

Chaok Seok and David W Oxtoby

Department of Chemistry and James Franck Institute, The University of Chicago, 5640 South Ellis Avenue, Chicago, IL 60637, USA

Received 9 May 1996, in final form 7 October 1996

**Abstract.** The equilibrium properties of the order–disorder transition in  $\text{Cu}_3\text{Au}$  have been studied using a density functional approach. A lattice analogue of density functional theory is employed with a mean-spherical approximation and nearest-neighbour pair and three-body potentials. We obtain surface transition and segregation similar to the experimental results for a range of parameters. A continuous surface transition occurs due to a smaller number of surface neighbours or weaker surface interactions than bulk ones. Surface segregation results from the different interaction potentials for different species. Our density functional approach is compared to a simple mean-field approach. The interesting dynamics of the transition may be studied in the future on the basis of our results.

## 1. Introduction

$\text{Cu}_3\text{Au}$  is a classic example of a binary system that exhibits a first-order order–disorder transition. It has a face-centred cubic lattice composed of four simple cubic sublattices (see figure 1(a)). In the perfectly ordered phase, one of the four sublattices is occupied by gold atoms and the other three by copper (see figure 1(b)). In the disordered state, gold and copper atoms are randomly distributed over the lattice sites.  $\text{Cu}_3\text{Au}$  is ordered at low temperature, and abruptly disorders at the transition temperature (663 K). However, short-range order persists above the transition temperature, and can be described by correlation functions. The equilibrium bulk order parameter has been measured [1, 2], and the ordering kinetics, such as nucleated and continuous ordering [3] or the scaling properties of late-stage ordering [4], has been studied.

The surface properties of this alloy have also been investigated using surface-sensitive techniques such as LEED [5, 6], low-energy ion scattering (LEIS) [7], x-ray scattering [8, 9], and helium-atom scattering [10]. In the [001] direction, which we focus on in this study, there are two kinds of alternating plane. In the ordered state, one kind of plane consists of a Cu sublattice and a Au sublattice (a Cu–Au layer), and the other planes of two Cu sublattices (Cu layers) as in figure 1(b). It is known that the outermost (001) surface in  $\text{Cu}_3\text{Au}$  is a Cu–Au layer. It has been found that this surface undergoes a second-order transition whereas the bulk transition is first order, and that gold atoms segregate at the surface over a large temperature range above the transition temperature. Some experimental results are shown in figure 2. Evolution of surface order with time upon quenching the sample has also been studied.

Various theories such as Landau theory [11], mean-field theory [12, 13], Monte Carlo calculations [5, 14], and the cluster variation method [15] have been applied to the order–disorder transition problem. Landau theory uses a polynomial expansion for the free energy

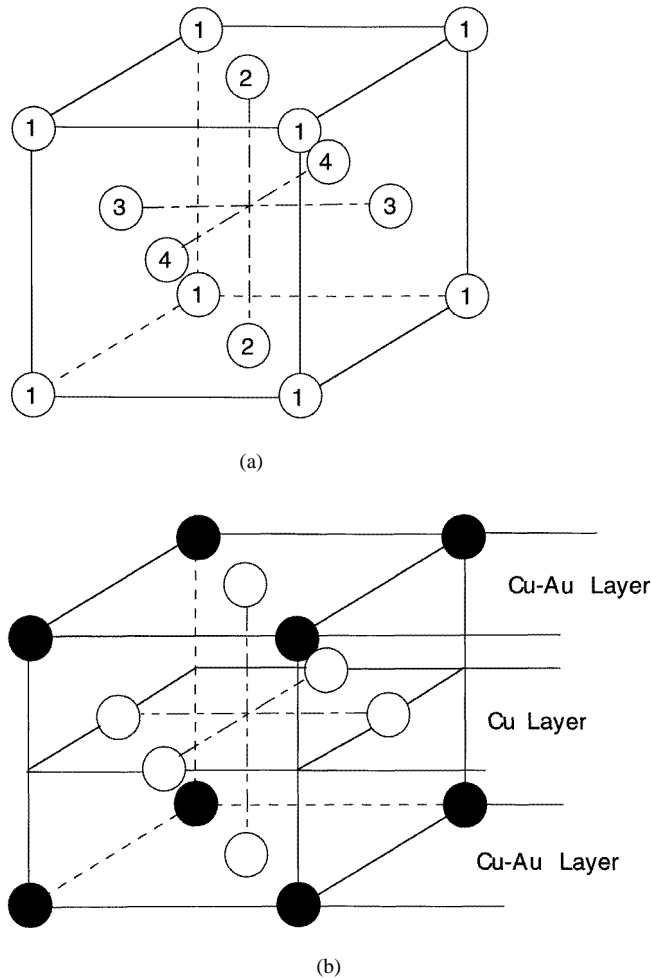


**Figure 1.** (a) A unit cell of an fcc lattice. The labels in the circles denote four sublattices. (b) Ordered  $\text{Cu}_3\text{Au}$  with a (001) surface. Black circles denote Au sites and white circles Cu sites. The top layer is the (001) surface.

which is simple, but does not include atomic details of a real system. The other theories begin with more realistic systems, but are more complex.

In this paper, we apply the lattice analogue of density functional theory, developed by Dieterich and co-workers [16], to the two-component system  $\text{Cu}_3\text{Au}$ . We calculate the equilibrium order parameter and composition profiles for a system with a (001) surface. In our density functional approach, the free energy is calculated from the interaction potentials and the lattice structure, but the calculation is relatively simple, so the theory can easily be extended to a study of dynamics, just as continuous density functional theories have been applied to the dynamics of liquid-crystal and gas-liquid transitions. Interesting problems such as whether ordering or disordering begin in the bulk or at the surface and how the velocity of growth of one phase in the other phase changes with temperature can be studied using our results as a starting point.

The outline of this paper is as follows. In section 2 the lattice analogue of density

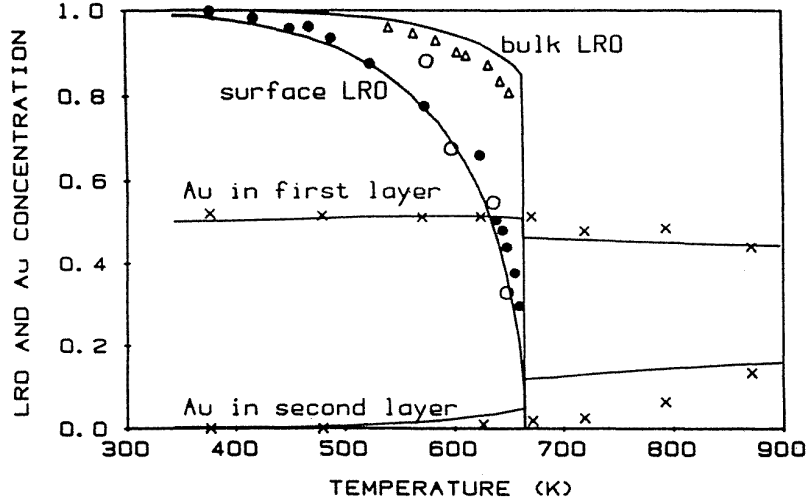


**Figure 2.** Experimental and calculated results from reference [15]: triangles, the long-range-order parameter in the bulk [2]; open and closed circles, the surface long-range-order parameter, from [5] and [6]; crosses, the Au concentration [7]; full lines, from the calculation using the cluster variation method [15].

functional theory (DFT) is reviewed, and in section 3 the direct correlation functions which are inputs in DFT are obtained. Sections 4 and 5 present the results for the bulk and surface transitions. In section 6 DFT is compared to a simple mean-field theory. Section 7 shows the results obtained using the potential parameters from a bond-order simulation (BOS) model. Section 8 gives conclusions.

## 2. The lattice analogue of density functional theory

In the lattice analogue of density functional theory, the grand canonical potential  $\Omega$  is a function of the occupation probabilities of the lattice sites, just as  $\Omega$  is a functional of the density in the continuous case [17]. For a two-component system,

$$\Omega(\{n_i^c, n_i^g\}) = \sum_i (\varepsilon_i^c n_i^c + \varepsilon_i^g n_i^g) + F(\{n_i^c, n_i^g\}) - \sum_i (\mu^c n_i^c + \mu^g n_i^g) \quad (1)$$

where subscripts denote lattice sites,  $i, j, \dots$ , and superscripts denote the kind of atom that occupies each lattice site,  $c$  for copper and  $g$  for gold for a  $\text{Cu}_3\text{Au}$  system. For example,  $n_i^c$  is the probability that a copper atom occupies site  $i$ .  $\varepsilon_i^v$  are external potentials and  $\mu^v$  are chemical potentials of species  $v$ .

$\Omega$  is minimized by a set of equilibrium occupation probabilities:

$$\left. \frac{\partial \Omega}{\partial n_i^v} \right|_{\{n_j^c, n_j^g\}_{eq}} = 0 \quad (2)$$

where  $v = c$  or  $g$ . The free energy  $F$  in equation (1) can be written as a sum of an ideal free energy and an excess free energy:

$$F = F_{id} + F_{exc} \quad (3)$$

$$F_{id} = -TS_{id} = kT \sum_i [n_i^c \ln n_i^c + n_i^g \ln n_i^g + (1 - n_i^c - n_i^g) \ln(1 - n_i^c - n_i^g)].$$

We approximate  $F_{exc}$  by expanding it around a reference state and truncating at second or third order. The third-order terms can be included approximately. By choosing a disordered state as a reference state, we obtain

$$F_{exc} = F_{exc,ref} - \beta^{-1} \sum_{v=c,g} \sum_i c_1^v \Delta n_i^v - \frac{\beta^{-1}}{2!} \sum_{v,\mu=c,g} \sum_{i,j} c_2^{v\mu}(i,j) \Delta n_i^v \Delta n_j^\mu - \frac{\beta^{-1}}{3!} \sum_{v,\mu,\lambda=c,g} \sum_{i,j,k} c_3^{v\mu\lambda}(i,j,k) \Delta n_i^v \Delta n_j^\mu \Delta n_k^\lambda \quad (4)$$

where  $\Delta n_i^v = n_i^v - n^v$ , and  $n^c$  and  $n^g$  without subscripts are the occupation probabilities for the disordered state. The one-, two-, and three-particle direct correlation functions for the reference state  $c_1^v$ ,  $c_2^{v\mu}(i,j)$ , and  $c_3^{v\mu\lambda}(i,j,k)$  are derivatives of the excess free energy evaluated at the reference state:

$$\begin{aligned} c_1^v &= -\beta \frac{\partial F_{exc}}{\partial n_i^v} \\ c_2^{v\mu}(i,j) &= -\beta \frac{\partial^2 F_{exc}}{\partial n_i^v \partial n_j^\mu} \\ c_3^{v\mu\lambda}(i,j,k) &= -\beta \frac{\partial^3 F_{exc}}{\partial n_i^v \partial n_j^\mu \partial n_k^\lambda}. \end{aligned} \quad (5)$$

$c_1^v(i)$  are site independent, so the argument 'i' is omitted.

The direct correlation functions  $c_2^{v\mu}(i,j)$  can be shown to be related to the pair correlation functions  $g^{v\mu}(i,j)$  via the lattice analogue of the Ornstein-Zernike equation:

$$g^{v\mu}(i,j) - 1 = C^{v\mu}(i,j) + \sum_{\lambda=c,g} \sum_k n_k^\lambda C^{v\lambda}(i,k) [g^{\lambda\mu}(k,j) - 1] \quad (6)$$

with

$$C^{v\mu}(i,j) = c_2^{v\mu}(i,j) - \frac{\delta_{ij}}{1 - n_i^c - n_i^g}. \quad (7)$$

The term  $\delta_{ij}/(1 - n_i^c - n_i^g)$  arises from the fact that a hard-core repulsion is taken into account from the outset in the lattice model.

In the limit where the vacancy probabilities  $(1 - n_i^c - n_i^g)$  are assumed to be zero, the above formalism for a two-component system reduces to that for a one-component system. The limit must be taken carefully, to cancel out infinities such as would appear in the second term of equation (7). For a bulk system,

$$\begin{aligned} \Omega &= \beta^{-1} \sum_i [n_i^c \ln n_i^c + (1 - n_i^c) \ln(1 - n_i^c)] - \beta^{-1} \sum_i (\beta \mu^c + c_1^c - \beta \mu^g - c_1^g) \Delta n_i^c \\ &\quad - \frac{\beta^{-1}}{2!} \sum_{i,j} A^{(2)}(i,j) \Delta n_i^c \Delta n_j^c \\ &\quad - \frac{\beta^{-1}}{3!} \sum_{i,j,k} A^{(3)}(i,j,k) \Delta n_i^c \Delta n_j^c \Delta n_k^c + \text{constants} \end{aligned} \quad (8)$$

where  $A^{(2)}(i,j)$  and  $A^{(3)}(i,j,k)$  are effective pair and three-body direct correlation functions for the effective one-component system:

$$\begin{aligned} A^{(2)}(i,j) &= c_2^{cc}(i,j) + c_2^{gg}(i,j) - 2c_2^{cg}(i,j) \\ A^{(3)}(i,j,k) &= c_3^{ccc}(i,j,k) - 3c_3^{cgg}(i,j,k) + 3c_3^{ggg}(i,j,k) - c_3^{ggg}(i,j,k). \end{aligned} \quad (9)$$

The term  $(\beta\mu^c + c_1^c - \beta\mu^g - c_1^g)$  in equation (8) can be expressed in terms of the occupation numbers of the reference state using the fact that the disordered state corresponds to a local or global minimum in the grand canonical potential surface, which is true above the lower spinodal temperature:

$$(\beta\mu^c + c_1^c - \beta\mu^g - c_1^g) = \ln(n^c/n^g). \quad (10)$$

Formal solutions for the equilibrium occupation numbers are obtained using equations (2), (8), and (10):

$$n_i^c = \left[ 1 + \frac{n^g}{n^c} \exp \left\{ - \sum_j A^{(2)}(i, j) \Delta n_j^c - \frac{1}{2} \sum_{j,k} A^{(3)}(i, j, k) \Delta n_j^c \Delta n_k^c \right\} \right]^{-1} \quad (11)$$

$$n_i^g = 1 - n_i^c.$$

The direct correlation functions are evaluated using a mean-spherical approximation (MSA) with the use of a nearest-neighbour interaction model. The inputs to our approach are then the properties of the disordered state (occupation probabilities and interaction potentials), and the outputs are properties of the transition such as the bulk and surface transition temperature, occupation probabilities for the ordered states, and surface profiles and free energies.

### 3. Direct correlation functions

A mean-spherical approximation is used to calculate the direct correlation functions  $c_2^{v\mu}(i, j)$  and  $c_3^{v\mu\lambda}(i, j, k)$  for the disordered state from the interaction potentials. It corresponds to replacing the direct correlation function by its asymptotic form. When only pair interactions are considered,

$$\begin{aligned} c_2^{v\mu}(i, j) &= -\beta v_2^{v\mu}(i, j) & i \neq j \\ g^{v\mu}(i, i) &= 0. \end{aligned} \quad (12)$$

With the nearest-neighbour potential model,

$$\begin{aligned} c_2^{v\mu}(i, j) &= -\beta v^{v\mu} & |\mathbf{r}_i - \mathbf{r}_j| = r_{NN} \\ c_2^{v\mu}(i, j) &= 0 & |\mathbf{r}_i - \mathbf{r}_j| > r_{NN} \end{aligned} \quad (13)$$

where  $r_{NN}$  is the nearest-neighbour distance and  $v^{v\mu}$  are the pair potentials between species  $v$  and  $\mu$  at that distance. The  $c_2^{v\mu}(i, i)$  are calculated using the above conditions and the Ornstein–Zernike equation analogue, equation (7). As a result, the direct correlation function  $A^{(2)}(i, j)$  in equation (9) is expressed as follows:

$$A^{(2)}(i, j) \equiv A^{(2)}(1) = c_2^{cc}(1) + c_2^{gg}(1) - 2c_2^{cg}(1) = -\beta V^{(2)} \quad |\mathbf{r}_i - \mathbf{r}_j| = r_{NN} \quad (14)$$

with

$$V^{(2)} = v^{cc} + v^{gg} - 2v^{cg}. \quad (15)$$

$A^{(2)}(i, i)$  is calculated from equation (7) by setting  $i = j$  and taking a linear combination of the four equations with  $v, \mu = c$  or  $g$ :

$$A^{(2)}(i, i) \equiv A^{(2)}(0) = c_2^{cc}(0) + c_2^{gg}(0) - 2c_2^{cg}(0) = -12 \frac{n^c}{1 - n^c} h^{cc}(1) A^{(2)}(1) \quad (16)$$

where  $h^{cc}(i, j) = g^{cc}(i, j) - 1$ , and the argument ‘1’ is used if the lattice sites  $i$  and  $j$  are nearest neighbours, and ‘0’ if  $i = j$ . Note that the term  $\delta_{ij}/(1 - n_i^c - n_i^g)$  is cancelled out by the linear combination.  $h^{cg}(1)$ ,  $h^{gc}(1)$ , and  $h^{gg}(1)$  are eliminated using

$n^c h^{vc}(i, j) + n^g h^{vg}(i, j) = 0$  and  $h^{cg}(i, j) = h^{gc}(i, j)$  in deriving equation (16).  $h^{cc}(1)$  is obtained from Fourier transformation of the Ornstein–Zernike equation analogue for a two-component system, solving the linear equations and taking the zero-vacancy limit:

$$h^{cc}(\mathbf{k}) = \frac{-1 + (1 - n^c)A^{(2)}(\mathbf{k})}{1 - n^c(1 - n^c)A^{(2)}(\mathbf{k})}. \quad (17)$$

The above equations (16) and (17) are solved iteratively to get self-consistent values of  $A^{(2)}(0)$ .

When three-body interactions are included, the two-body direct correlation functions are still assumed to be given by equation (16). Equation (13) is extended to the three-body correlation functions such that  $c_3^{v\mu\lambda}(i, j, k) = -\beta v_3^{v\mu\lambda}(i, j, k)$  if  $i, j$ , and  $k$  are all nearest neighbours.  $c_3^{v\mu\lambda}(i, i, j)$  and  $c_3^{v\mu\lambda}(i, i, i)$  are assumed to be zero, which corresponds to a simple mean-field approach (see section 6). Then,

$$\begin{aligned} A^{(3)}(i, j, k) &\equiv A^{(3)}(1) = -\beta V^{(3)} && \text{if } i, j, k \text{ are NN} \\ A^{(3)}(i, j, k) &= 0 && \text{otherwise} \end{aligned} \quad (18)$$

with

$$V^{(3)} = v^{ccc} - 3v^{cgg} + 3v^{cgg} - v^{ggg}. \quad (19)$$

#### 4. Bulk transition

We now apply the density functional theory with the direct correlation functions from section 3 to the bulk transition of  $\text{Cu}_3\text{Au}$ .

From equation (11), the occupation probabilities in the ordered state are expressed as follows:

$$n_i^c = \left[ 1 + \frac{n^g}{n^c} \exp(-\beta \epsilon_i^c) \right]^{-1}$$

where

$$\begin{aligned} \beta \epsilon_c^c &= A^{(2)}(0) \Delta n_c^c + A^{(2)}(1)(4 \Delta n_g^c + 8 \Delta n_c^c) + 8A^{(3)}(1)(2 \Delta n_g^c \Delta n_c^c + \Delta n_c^c \Delta n_c^c) \\ \beta \epsilon_g^c &= A^{(2)}(0) \Delta n_g^c + 12A^{(2)}(1) \Delta n_c^c + 24A^{(3)}(1) \Delta n_c^c \Delta n_c^c. \end{aligned} \quad (20)$$

$\epsilon_i^c$  are effective external potentials due to the interparticle interactions. Note that there are two kinds of distinctive site in the ordered states: copper ( $i = c$ ) and gold ( $i = g$ ).

Equilibrium occupation probabilities and the free energy  $\Omega$  are calculated as functions of  $A^{(2)}(1)$ , which is proportional to the inverse of the absolute temperature in the MSA. The occupation probabilities are obtained numerically by an iterative procedure using

$$(n_\lambda^v)_{i+1} = (n_\lambda^v)_i - d \left. \frac{\partial \Omega}{\partial n_\lambda^v} \right|_{\{n_\lambda^v\}_i} \quad (21)$$

where  $d$  is chosen to get a fast convergence. The transition temperature is determined by setting the values of  $\Omega$  for the ordered and the disordered states equal.

Let us consider first the case in which the three-body potentials are set to zero. The result obtained numerically is that the bulk undergoes a first-order transition, as can be seen from figure 3, and the transition point is

$$A_{tr}^{(2)}(1) = -\beta_{tr}(v^{cc} + v^{gg} - 2v^{cg}) = -4.00. \quad (22)$$

The order parameter in the figure is defined as the difference between the probability that a Cu atom occupies a correct site (in terms of the perfectly ordered state) and the probability

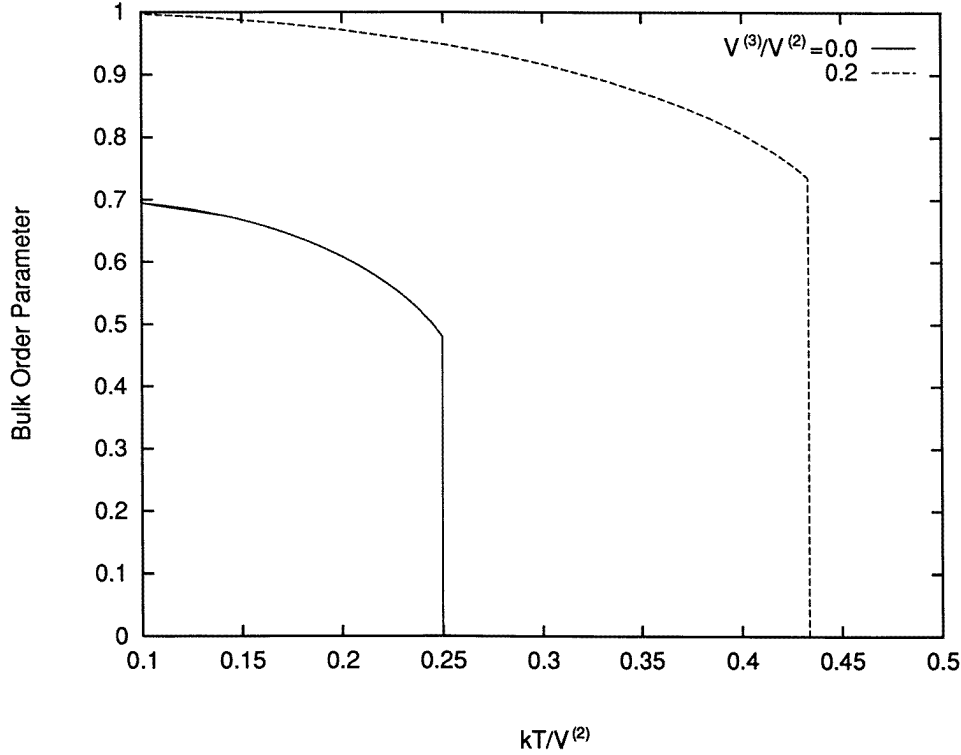


**Figure 3.** The bulk order parameter versus  $kT/V^{(2)}$ . The solid curve represents the pair-interactions-only case, and the dashed curve the case with three-body interactions.

that it occupies a wrong site. For bulk, the order parameter is  $(n_c^c - n_g^c)$ . From equation (22),  $V^{(2)} = v^{cc} + v^{gg} - 2v^{cg}$  should be positive in order for the order–disorder transition to occur. In other words, the average attractive interactions between like species should be weaker than those between unlike species. The ordered state obtained by using only two-body interactions is a little disordered even at low temperatures, because a perturbation theory at a low order has been used.

Inclusion of three-body terms produces improved results (the dashed line in figure 3). In this case, the transition temperature is a function of both  $A^{(2)}(1)$  and  $A^{(3)}(1)/A^{(2)}(1) = V^{(3)}/V^{(2)}$ . The transition temperature increases, and the ordered states become more ordered for a given  $V^{(2)}$  as  $V^{(3)}/V^{(2)}$  increases, because the system has an additional driving force for ordering.

## 5. Surface transition

The equilibrium profiles in the presence of a free surface can be obtained by minimizing  $\Omega$  under the following boundary conditions:

$$\begin{aligned} n_{\lambda,l}^v &\longrightarrow 0 & l &\longrightarrow -\infty \\ n_{\lambda,l}^v &\longrightarrow n_{\lambda}^v(\text{bulk}) & l &\longrightarrow \infty \end{aligned} \quad (23)$$



where  $l$  is layer number. We consider a half-infinite system with a (001) surface. Cu–Au layers have equal numbers of copper and gold sites, and the order parameters are  $n_{c,l}^c - n_{g,l}^c$  (see figure 1(b)). Cu layers have copper sites only, and the order parameters for these layers are not defined. We can have both kinds of surface layer as boundary conditions, and choose the layer which gives the lower surface free energy as the equilibrium surface layer.

A proper reference state for the surface problem is needed in the density functional approach. The disordered bulk is used as a reference state as in the bulk transition calculations in section 5.1, and a system with a surface is used in section 5.2.

### 5.1. The disordered bulk reference state

The same reference state as is used in section 3 is used in this section, although the expansion of a surface system around a bulk state may not be a good approximation.

If there exists a surface,  $\Omega$  differs from equation (8) by a surface field and a surface enhancement which arises formally from the correlations between the vacuum and the surface layer:

$$\begin{aligned} \Omega = & \beta^{-1} \sum_i [n_i^c \ln n_i^c + (1 - n_i^c) \ln(1 - n_i^c)] - \beta^{-1} \sum_i (\ln(n^c/n^g) - \beta F(i)) \Delta n_i^c \\ & - \frac{\beta^{-1}}{2!} \sum'_{i,j} (A^{(2)}(i,j) - \beta I(i,j)) \Delta n_i^c \Delta n_j^c \\ & - \frac{\beta^{-1}}{3!} \sum'_{i,j,k} A^{(3)}(i,j,k) \Delta n_i^c \Delta n_j^c \Delta n_k^c \end{aligned} \quad (24)$$

where  $\sum'$  stands for a summation over *occupied* lattice sites. The surface field  $F(i)$  is non-zero (equal to  $F$ ) only if the lattice site  $i$  is on the surface layer, and the surface interaction  $I(i,j)$  is non-zero (defined as  $I$ ) only if  $i$  and  $j$  are nearest neighbours both on the surface layer:

$$\begin{aligned} F = & -4[n^c(v^{cc} - v^{cg}) + n^g(v^{cg} - v^{gg})] \\ & + 4[n^c n^c(v^{ccc} - v^{cgg}) + 2n^c n^g(v^{cgg} - v^{ggg}) + n^g n^g(v^{ggg} - v^{ggg})] \end{aligned} \quad (25)$$

$$I = -2[n^c(v^{ccc} - 2v^{cgg} + v^{ggg}) + n^g(v^{cgg} - 2v^{ggg} + v^{ggg})]. \quad (26)$$

If the surface field  $F > 0$ ,  $\Omega$  will be lowered by the smaller  $\Delta n_i^c$  for the site  $i$  at the surface, as can be seen from equation (24). As a result, gold segregates at the surface if  $F > 0$ , and copper segregates if  $F < 0$ . In other words, strong Cu–Cu (or Cu–Au) interactions compared to Cu–Au (or Au–Au) interactions which make  $F$  positive favour Au at the surface because surface atoms have a smaller number of neighbours. If the surface enhancement  $I > 0$ , the surface atoms have stronger effective pair interactions, and tend to be more ordered. The opposite is true if  $I < 0$ . Numerical calculations show that the magnitude of  $F$  affects the ordering of the surface to some degree, greater  $|F|$  increasing the surface order, while the effect of  $I$  on surface segregation is small.

With no surface field and surface enhancement the surface transition is second order and occurs below the bulk transition temperature as in the calculations using the cluster variation method [18]. Depending on the surface parameters, the surface transition can be second order with varying transition temperatures, or first order with the same transition point as the bulk. If only pair interactions are included,  $F/V^{(2)}$  is the only parameter. If it is varied to give a second-order surface transition near the bulk transition temperature, very little Au segregation occurs, and the surface order parameter is much smaller than the

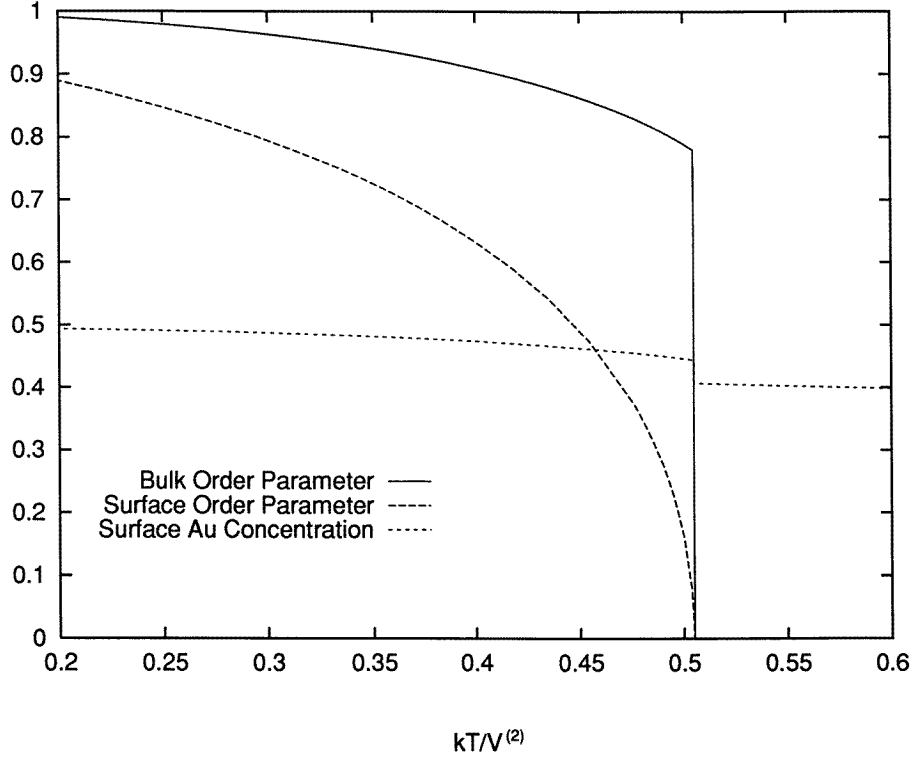


**Figure 4.** The density functional calculation results with a bulk reference for the bulk and surface transition for a system with  $V^{(3)}/V^{(2)} = 0.3$ ,  $F/V^{(2)} = 0.9$ , and  $I/V^{(2)} = -0.0805$ .

bulk value. The poor results on the surface problem without three-body interactions are not surprising in view of the bulk transition results in section 3. When three-body interactions are included, a surface transition and surface segregation similar to the experimental results can be obtained if  $F$  is large enough to give surface Au segregation, and  $I$  is varied to have the same bulk and surface transition temperature. An example is shown in figure 4 for a set of parameters that gives surface segregation of Au and a surface transition near the bulk transition temperature. The overall agreement with the experimental data in figure 2 is good, although the surface order parameter does not approach the bulk rapidly enough at low  $T$ . The surface segregation profiles in figure 5 show exponential decays of the segregation with layer number above the transition temperatures as in reference [9]. Although the amplitude of the calculated profile is smaller than the experimental data for the particular choice of the parameters, the shape and the range of the oscillation are similar. The surface order parameter profiles are shown in figure 6.

### 5.2. The reference state with a surface

A half-infinite system which is completely disordered, and has constant layer composition ( $n^c$  for all layers = 0.75) is chosen as an alternative reference state for the surface problem. In this case, the term  $(\beta\mu^c + c_1^c(i) - \beta\mu^s - c_1^s(i))$  and  $A^{(2)}(0)$  depend on layer number since the translational symmetry is broken in the direction perpendicular to the surface. We

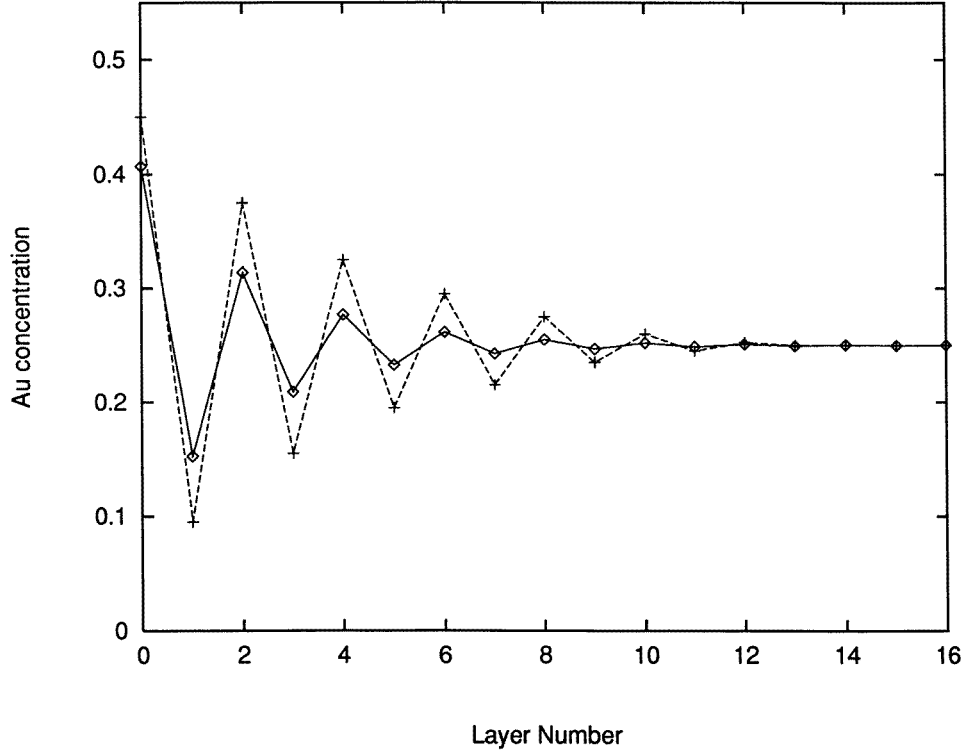


**Figure 5.** The surface segregation profile at  $A^{(2)}(1) = -1.98$  (the solid line), which is just above the transition temperature  $A_{Tr}^{(2)}(1) = -1.9801$ , is compared to the experimental data for  $T_r + 1$  K from reference [9] (the dashed line). The potential parameters used in the calculation are the same as in figure 4.

assume that only surface pair interactions are different from bulk.

Because the half-infinite system with constant layer composition is not generally an extremum of  $\Omega$ , equation (2) cannot be used for this reference state. We write the term  $(\beta\mu^c + c_1^c(i) - \beta\mu^g - c_1^g(i))$  as follows:

$$(\beta\mu^c + c_1^c(i) - \beta\mu^g - c_1^g(i)) = (\beta\mu^c + c_1^c - \beta\mu^g - c_1^g)_{bulk} + (c_1^c(i) - c_1^g(i)) - (c_1^c - c_1^g)_{bulk} = \ln(n^c/n^g) - \beta F'(i) \quad (27)$$

where equation (10) and the definition  $-\beta F'(i) = (c_1^c(i) - c_1^g(i)) - (c_1^c - c_1^g)_{bulk}$  are used.  $c_1^v(i)$  can be calculated by expanding it around a reference state. If the bulk disordered state is used as the reference,  $F'(i)$  is the same as  $F$  in subsection 5.1 where the bulk reference is used from the outset. In this subsection the following trick is used: get two equations by expanding  $c_{1,vacuum}^v$  around a bulk and a half-infinite system, and eliminate  $c_{1,vacuum}^v$  to get relations between  $c_{1,half-infinite}^v(i)$  and  $c_{1,bulk}^v$ . As a result,  $F'(i)$  is expressed as follows:

$$\begin{aligned} -\beta F'(i) = & -n^c \{c_{\infty}^{cc}(0) - c_{\infty}^{cg}(0)\} - n^g \{c_{\infty}^{cg}(0) - c_{\infty}^{gg}(0)\} \\ & + n^c \{c_0^{cc}(0) - c_0^{cg}(0)\} + n^g \{c_0^{cg}(0) - c_0^{gg}(0)\} \\ & - 4[2n^c \{c_2^{cc}(1) - c_2^{cg}(1)\} + 2n^g \{c_2^{cg}(1) - c_2^{gg}(1)\}] \\ & - n^c \{c_{2,surf}^{cc}(1) - c_{2,surf}^{cg}(1)\} - n^g \{c_{2,surf}^{cg}(1) - c_{2,surf}^{gg}(1)\} \end{aligned}$$

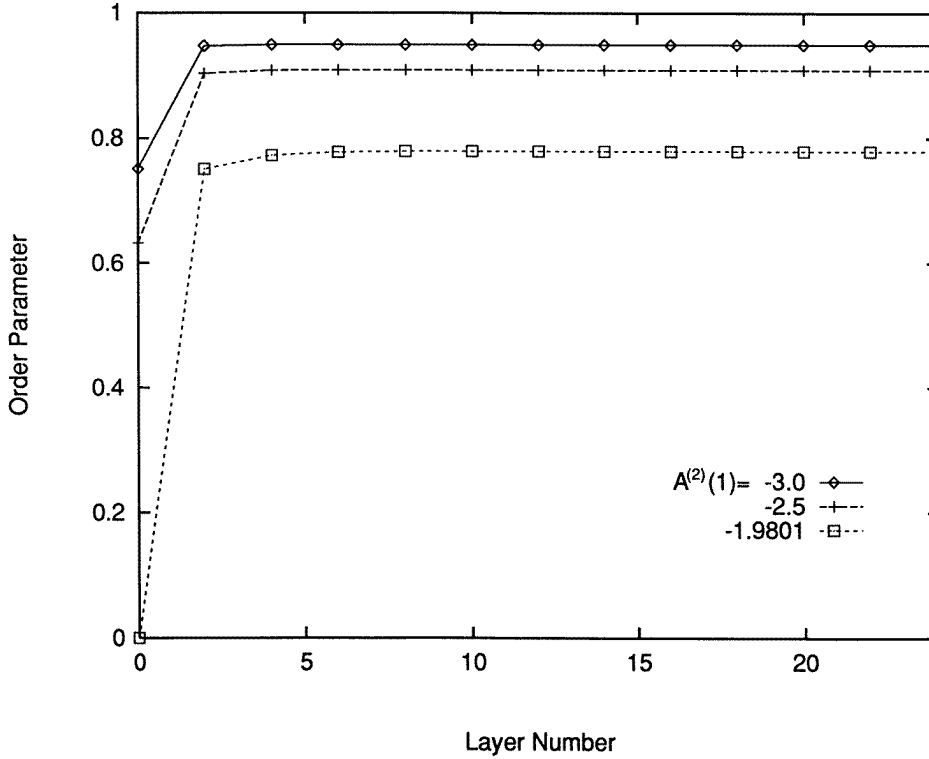


**Figure 6.** Surface order parameter profiles at temperatures below the transition temperature  $A_{lr}^{(2)}(1) = -1.9801$ . The potential parameters used are the same as in figure 4.

$$\begin{aligned}
 &+ 12[n^c n^c \{c_3^{ccc}(1) - c_3^{ccg}(1)\} + 2n^c n^g \{c_3^{ccg}(1) - c_3^{cgg}(1)\} \\
 &+ n^g n^g \{c_3^{cgg}(1) - c_3^{ggg}(1)\}]
 \end{aligned} \quad (28)$$

for the site  $i$  at the surface. If  $i$  is at the  $l$ th layer, then

$$\begin{aligned}
 -\beta F'(i) = & -n^c \{c_\infty^{cc}(0) - c_\infty^{cg}(0)\} - n^g \{c_\infty^{cg}(0) - c_\infty^{gg}(0)\} \\
 & + n^c \{c_l^{cc}(0) - c_l^{cg}(0)\} + n^g \{c_l^{cg}(0) - c_l^{gg}(0)\}.
 \end{aligned} \quad (29)$$

Note that the  $c_2^{v\mu}(0)$  are layer dependent, and so are represented by  $c_l^{v\mu}(0)$  where  $l$  is the layer number, and  $l = 0$  and  $l = \infty$  denote the surface layer and the bulk.  $F'(i)$  is different from  $F$  in equation (25) in that it includes the contribution from the surface interactions and  $c_2^{v\mu}(0)$ , and is not zero for layers other than the surface.

The bulk and layer  $c_2^{vc}(0) - c_2^{vg}(0)$  or  $A^{(2)}(0)$  are calculated by similar analysis to that in section 3 as follows:

$$c_\infty^{vc}(0) - c_\infty^{vg}(0) = -12 \frac{n^c}{1 - n^c} \{c_2^{vc}(1) - c_2^{vg}(1)\} h^{cc}(1) \quad (30)$$

$$\begin{aligned}
 c_l^{vc}(0) - c_l^{vg}(0) = & -4 \frac{n^c}{1 - n^c} [\{c_{l,l}^{vc}(1) - c_{l,l}^{vg}(1)\} h_{l,l}^{cc}(1) \\
 & + (1 - \delta_{l,0}) \{c_{l,l-1}^{vc}(1) - c_{l,l-1}^{vg}(1)\} h_{l,l-1}^{cc}(1) \\
 & + \{c_{l,l+1}^{vc}(1) - c_{l,l+1}^{vg}(1)\} h_{l,l+1}^{cc}(1)]
 \end{aligned} \quad (31)$$

$$A_l^{(2)}(0) = -4 \frac{n^c}{1-n^c} [A_{l,l}^{(2)}(1)h_{l,l}^{cc}(1) + (1-\delta_{l,0})A_{l,l-1}^{(2)}(1)h_{l,l-1}^{cc}(1) + A_{l,l+1}^{(2)}(1)h_{l,l+1}^{cc}(1)] \quad (32)$$

where  $c_{l,l'}^{v\mu}(1)$  and  $h_{l,l'}^{cc}(1)$  are correlation functions between two atoms in layers  $l$  and  $l'$ . The  $h_{l,l'}^{cc}(1)$  are obtained from the layer-dependent  $h_l^{cc}(\mathbf{k})$ :

$$\begin{aligned} h_l^{cc}(\mathbf{k}) = & [1 - n^c(1 - n^c)\{A_l^{(2)}(0) + A_{l,l}^{(2)}(1)f_{xy}(\mathbf{k})\}]^{-1} \\ & \times [-1 + (1 - n^c)\{A_l^{(2)}(0) + A_{l,l}^{(2)}(1)f_{xy}(\mathbf{k}) \\ & + A_{l,l-1}^{(2)}(1)f_{-z}(\mathbf{k})(1 + (1 - \delta_{l,0})n^c h_{l-1}^{cc}(\mathbf{k})) \\ & + A_{l,l+1}^{(2)}(1)f_{+z}(\mathbf{k})(1 + n^c h_{l+1}^{cc}(\mathbf{k}))\}] \end{aligned} \quad (33)$$

where

$$\begin{aligned} f_{xy}(\mathbf{k}) &= 4 \cos(k_x a/2) \cos(k_y a/2) \\ f_{-z}(\mathbf{k}) &= 2e^{-ik_z a/2} \{\cos(k_x a/2) \cos(k_y a/2)\} \\ f_{+z}(\mathbf{k}) &= 2e^{ik_z a/2} \{\cos(k_x a/2) \cos(k_y a/2)\}. \end{aligned}$$

The case where only the surface correlation function  $A_{0,0}^{(2)}(1) = -\beta V_{surf}^{(2)}$  is different from the bulk correlation function  $A^{(2)}(1) = -\beta V^{(2)}$  is considered.

Gold segregation is obtained if  $F'$  at the surface is positive as in the previous subsection. The surface term in  $F'$  is positive if the surface Au–Au (Cu–Au) interaction is stronger than the Cu–Au (Cu–Cu) interaction. If  $F'$  is large enough to give significant Au segregation,  $V_{surf}^{(2)}$  should be smaller than  $V^{(2)}$  in order to give a second-order surface transition. We find similar results on surface transition, surface segregation and order parameter profiles to those in figures 4, 5 and 6.

## 6. A simple mean-field approach

The density functional approach presented in sections 4 and 5 is a mean-field approach in the sense that it does not allow fluctuations, but it is more sophisticated than usual mean-field approaches. Here we compare the density functional approach with a simple mean-field approach.

The grand canonical potential  $\Omega$  can be written as follows within a mean-field approximation:

$$\begin{aligned} \Omega_{MF} = & \beta^{-1} \sum_i [n_i^c \ln n_i^c + n_i^g \ln n_i^g + (1 - n_i^c - n_i^g) \ln(1 - n_i^c - n_i^g)] - \sum_{v=c,g} \sum_i \mu^v n_i^v \\ & + \frac{1}{2!} \sum_{v,\mu=c,g} \sum_{i,j} v^{v\mu}(i,j) n_i^v n_j^\mu + \frac{1}{3!} \sum_{v,\mu,\lambda=c,g} \sum_{i,j,k} v^{v\mu\lambda}(i,j,k) n_i^v n_j^\mu n_k^\lambda \end{aligned} \quad (34)$$

where the configurational entropy for the non-interacting system and the assumption

$$g^{v\mu}(i,j) = g_3^{v\mu\lambda}(i,j,k) = 1 \quad (35)$$

are employed. The chemical potentials can be obtained by using equation (2) for the disordered state:

$$\begin{aligned} \mu^c - \mu^g = & \beta^{-1} \ln(n^c/n^g) + 12n^c(v^{cc} - v^{cg}) + 12n^g(v^{cg} - v^{gg}) \\ & + 24n^c n^c(v^{ccc} - v^{cgg}) + 48n^c n^g(v^{cgg} - v^{ggg}) + 24n^g n^g(v^{cgg} - v^{ggg}) \end{aligned} \quad (36)$$

where the nearest-neighbour pair and three-body interaction model is used as in the above density functional approach.

$\Omega_{MF}$  can be compared to  $\Omega_{DF}$  by expanding  $\Delta n_i^v$  in  $\Omega_{DF}$ . The following correspondences are found for the correlation functions in  $\Omega_{DF}$  and the potential parameters in  $\Omega_{MF}$ :

$$\begin{aligned} c_2^{v\mu}(1) - 4n^c c_3^{v\mu c}(1) - 4n^g c_3^{v\mu g}(1) &\longleftrightarrow -\beta v^{v\mu} \\ c_2^{v\mu}(0) &\longleftrightarrow 0 \\ c_3^{v\mu\lambda}(1) &\longleftrightarrow -\beta v^{v\mu\lambda}. \end{aligned} \quad (37)$$

Note that  $c_2^{v\mu}(0) = 0$  corresponds to the assumption in equation (35) (see equation (16)).

For a system with a surface,  $\Omega_{DF}$  with the bulk reference state reduces to  $\Omega_{MF}$  with equation (37).  $\Omega_{DF}$  with a surface reference reduces to  $\Omega_{MF}$  with equation (37) and the following:

$$c_{2,surf}^{v\mu}(1) - 2n^c c_3^{v\mu c}(1) - 2n^g c_3^{v\mu g}(1) \longleftrightarrow -\beta v_{surf}^{v\mu}. \quad (38)$$

Equation (38) is different from the first line in equation (37) because there are two lattice sites with which a given nearest-neighbour (NN) pair makes NN triple whereas there are four for a bulk pair.

If only pair interactions are considered,  $\Omega_{MF}$  is the same as  $\Omega_{DF}$  within the MSA except  $A^{(2)}(0)$ . The bulk transition temperature is

$$-\beta_{tr}(v^{cc} + v^{gg} - 2v^{cg}) = -1.21 \quad (39)$$

which is higher than that from the density functional calculation. When the second-order surface transition occurs at the bulk transition temperature, there is almost no surface segregation above the transition temperature, and the bulk transition curve shows large curvature near the transition temperature.

When three-body interactions are included, the notation  $V_{MF}^{(2)}$ ,  $V_{MF}^{(3)}$ ,  $F_{MF}$ , and  $I_{MF}$  together with equation (37) are used. For example,

$$V_{MF}^{(2)} = (v^{cc} + v^{gg} - 2v^{cg}) + 4n^c(v^{ccc} + v^{cgg} - 2v^{c cg}) + 4n^g(v^{c cg} + v^{ggg} - 2v^{c gg}). \quad (40)$$

Those parameters have similar effects on the surface transition to those in the density functional case. When the second-order surface transition occurs at the bulk transition temperature, the transition curves are similar to those in figure 4, but the bulk order parameter is somewhat too small at the transition temperature relative to experiment.

## 7. Potentials from the BOS model

In this section, we use the interaction potentials obtained from the parameters in the bond-order simulation (BOS) model [19] to study bulk and surface transitions. The BOS parameters have been determined from the mixing energies for bimetallic systems of different compositions, and used to predict the structures of bimetallic clusters.

In the BOS model, the site energy for an A-type atom surrounded by  $M$  of B type is expressed as

$$\epsilon_{Z,M \text{ of } B}^A = \epsilon_Z^A + M \Delta E_{Z,A-B}^A + \frac{M(M-1)}{2} \lambda_{Z,A-B}^A \quad (41)$$

and likewise for the site energy for a B-type atom.  $Z$  is the number of neighbours around a given atom,  $\epsilon_Z^A = \epsilon_{Z,M=0}^A$ , and  $\Delta E_{Z,A-B}^A$  is the bond-change energy when one of the  $Z$  neighbours of atom A is replaced by a B atom. The first bond change  $\Delta E_{Z,A-B}^A$  is constant,

but the subsequent bond-change energies are different due to the many-body effect, and are included in the third term of the right-hand side of equation (41).

The bulk potential parameters that we need are extracted from the following relations, which can be derived by considering the changes in the numbers and kinds of pair and three-body interactions when one of the surrounding atoms is replaced by the other type:

$$\begin{aligned}
\epsilon_{12}^c/12 &= (1/2)(v^{cc}) + (n/6)(v^{ccc}) \\
\epsilon_{12}^g/12 &= (1/2)(v^{gg}) + (n/6)(v^{ggg}) \\
\Delta E_{12}^c &= (1/2)(v^{cg} - v^{cc}) + (n/3)(v^{cgg} - v^{ccc}) \\
\Delta E_{12}^g &= (1/2)(v^{cg} - v^{gg}) + (n/3)(v^{cgg} - v^{ggg}) \\
11\lambda_{12}^c &= -(n/3)(v^{cgg} - v^{ccc}) + (n/3)(v^{cgg} - v^{cgg}) \\
11\lambda_{12}^g &= -(n/3)(v^{cgg} - v^{ggg}) + (n/3)(v^{cgg} - v^{cgg})
\end{aligned} \tag{42}$$

where  $n$  is the number of triples including a given central atom which are changed by the replacement of one of the atoms surrounding the central one by the other type, and is equal to 4 for an fcc lattice.

The surface interaction potentials are obtained from the following equations. We use

$$\begin{aligned}
\Delta E_8^c &= (1/4)(v_{surf}^{cg} - v_{surf}^{cc}) + (1/4)(v^{cg} - v^{cc}) + (n/4)(v^{cgg} - v^{ccc}) \\
\Delta E_8^g &= (1/4)(v_{surf}^{cg} - v_{surf}^{gg}) + (1/4)(v^{cg} - v^{gg}) + (n/4)(v^{cgg} - v^{ggg}) \\
\Delta E_8^c + \Delta E_8^g &= \Delta E_{12}^c + \Delta E_{12}^g.
\end{aligned} \tag{43}$$

to get  $V_{surf}^{(2)}$ , and

$$\begin{aligned}
\epsilon_8^c/4 &= (1/2)(v_{surf}^{cc}) + (1/2)(v^{cc}) + (3n/12)(v^{ccc}) \\
\epsilon_8^g/4 &= (1/2)(v_{surf}^{gg}) + (1/2)(v^{gg}) + (3n/12)(v^{ggg})
\end{aligned} \tag{44}$$

to get  $v_{surf}^{cc} - v_{surf}^{gg}$ .

Three sets of BOS parameters from the experimental data at (a) 800 K and (b) 298 K, and from (c) a quantum chemical density functional calculation [20] are used to get the potential parameters. Those parameters are shown in table 1. The bulk transition temperatures calculated are (a) 124 K, (b) 655 K, and (c) 609 K. Note that the second is only 1.2% away from the experimental value, 663 K. The surface transitions obtained are different from the experimental results in figure 2, however. More ordered surfaces compared to the experimental results are obtained when either the bulk reference or the surface reference state are used. The most important discrepancy with experiment is that Cu segregates at the surface in either case because of the large negative surface field  $F$  or  $F'$ . The simple mean-field calculation of section 6 gives bulk transition temperatures around 370 K for all three sets of data, and Cu segregation.

## 8. Conclusions

The equilibrium properties of the order-disorder transition in  $\text{Cu}_3\text{Au}$  with a (001) surface have been studied using a lattice version of density functional theory. A continuous surface transition and oscillating surface segregation profiles are obtained for a range of potential parameters, and the general shapes agree with experiment.

It is appropriate to compare the density functional approach to other theoretical methods. First, our approach can be reduced to a simple Landau theory by expanding the free energy as a power series in the order parameter, truncated at low order; this is unlikely to be correct

**Table 1.** The BOS parameters and the potential parameters.

Input to BOS	800 K	298 K	DFT
$\epsilon_{12}^c$ (eV)	−3.49	−3.49	−3.49
$\epsilon_{12}^g$ (eV)	−3.81	−3.81	−3.81
$\Delta E_{12,c-g}^c$ (kJ mol <sup>−1</sup> )	−2.02	−0.64	−0.74
$\Delta E_{12,c-g}^g$ (kJ mol <sup>−1</sup> )	0.56	1.93	1.84
$\lambda_{12,c-g}^c$ (kJ mol <sup>−1</sup> )	0.08	−0.42	−0.39
$\lambda_{12,c-g}^g$ (kJ mol <sup>−1</sup> )	−0.02	−0.52	−0.48
$V^{(2)}$ (kJ mol <sup>−1</sup> ) <sup>a</sup>	1.60	18.1	16.9
$V^{(3)}/V^{(2)}$ <sup>a</sup>	0.516	0.0456	0.0438
$F/V^{(2)}$ <sup>b</sup>	−11.2	−2.37	−2.38
$I/V^{(2)}$ <sup>b</sup>	−0.567	0.406	0.402
$F'_{surf}/V^{(2)}$ <sup>c</sup>	−9.80	−3.43	−3.34
$V^{(2)}_{surf}/V^{(2)}$ <sup>c</sup>	1.40	0.429	0.435
$V_{MF}^{(2)}$ (kJ mol <sup>−1</sup> ) <sup>d</sup>	3.42	3.42	3.33
$V_{MF}^{(3)}/V_{MF}^{(2)}$ <sup>d</sup>	0.242	0.242	0.223
$F_{MF}/V_{MF}^{(2)}$ <sup>d</sup>	−0.367	−1.17	−1.15
$I_{MF}/V_{MF}^{(2)}$ <sup>d</sup>	−0.266	2.15	2.05

<sup>a</sup> Used in the calculation of sections 5.1 and 5.2.

<sup>b</sup> Section 5.1.

<sup>c</sup> Section 5.2.

<sup>d</sup> Section 6.

near a first-order transition, however, and the continuum square-gradient approximation employed for an inhomogeneous system with a free surface will not be a good approximation to the actual lattice system except near a second-order transition where the order parameter changes slowly in space.

Second, we can compare our method with what we refer to as ‘simple mean-field’ theory in section 6 above. Our theory corresponds in structure to that approach, but is more accurate in predicting the transition temperature. It is also more flexible for future applications, as it is straightforward to generalize the mean-spherical approximation used here to a more sophisticated closure. One key question is that of why our theory (as well as the simple mean-field theory) give preferential copper segregation at the surface instead of gold, as is seen in experiment. Although we cannot prove that this is the case, we feel that the parameters of the BOS model, which are fitted to bulk heat of mixing data for the alloys, do not properly describe the nature of the surface, and that the problem therefore lies in the potential rather than in the theoretical approach. This hypothesis could be tested by Monte Carlo simulations of half-infinite systems using the BOS model.

Finally, one can compare our approach to other theoretical methods such as Monte Carlo simulations and the cluster variation method. These calculations are lengthier and less transparent physically. It is also not clear how to extend them to dynamical problems. We are currently using density functional theory to study bulk and surface nucleation in the  $\text{Cu}_3\text{Au}$  system using the equilibrium profiles obtained in this study as boundary conditions.

In view of the importance of three-body terms in our calculation, one might ask whether



four-body and higher terms also matter; that is, the expansion might be slowly convergent. In our view, the three-body terms provide the essential physical content as reflected in the statement that the interaction between two copper atoms, for example, is different at a surface, surrounded by other copper atoms, or surrounded by gold atoms. A three-body potential allows for this effect, while a four-body term would provide just a higher-order and less physically motivated correction. In order to go beyond the present approach, it would be necessary to use a still more sophisticated density functional theory based on a density- or occupation-dependent potential from quantum mechanical theories.

### Acknowledgments

This work was supported by the National Science Foundation through grant CHE 9422999 and through the Materials Research Science and Engineering Center at the University of Chicago.

### References

- [1] Keating D T and Warren B E 1951 *J. Appl. Phys.* **22** 286
- [2] Feder R, Mooney M and Nowick A S 1958 *Acta Metall.* **6** 266
- [3] Ludwig K F Jr, Stephenson G B, Jordan-Sweet J L, Mainville J, Yang Y S and Sutton M 1988 *Phys. Rev. Lett.* **61** 1859
- [4] Shannon R F Jr, Nagler S E, Harkless C R and Nicklow R M 1992 *Phys. Rev. B* **46** 40
- [5] Sundaram V S, Alben R S and Robertson W D 1974 *Surf. Sci.* **46** 653
- [6] McRae E G and Malic R A 1984 *Surf. Sci.* **148** 551
- [7] Buck T M, Wheatley G H and Marchut L 1983 *Phys. Rev. Lett.* **51** 43
- [8] Dosch H, Mailander L, Reichert H, Peisl J and Johnson R L 1991 *Phys. Rev. B* **43** 13 172
- [9] Reichert H, Eng P J, Dosch H and Robinson I K 1995 *Phys. Rev. Lett.* **74** 2006
- [10] King S F 1993 *PhD Thesis* University of Chicago
- [11] Lipowsky R and Speth W 1983 *Phys. Rev. B* **28** 3983  
Lipowsky R 1987 *Ferroelectrics* **73** 69
- [12] Kroll D M and Gomper G 1987 *Phys. Rev. B* **36** 7080
- [13] Mecke K M and Dietrich S 1995 *Phys. Rev. B* **52** 2107
- [14] Gomper G and Kroll D M 1988 *Phys. Rev. B* **38** 459
- [15] Sanchez J M and Mórán-López J L 1985 *Surf. Sci.* **157** L297
- [16] Nieswand M, Dieterich W and Majhofer A 1993 *Phys. Rev. E* **47** 718  
Nieswand M, Majhofer A and Dieterich W 1993 *Phys. Rev. E* **48** 2521
- [17] Oxtoby D W 1990 Crystallization of liquids; a density functional approach *Liquids, Freezing and Glass Transition* (Elsevier: Amsterdam)
- [18] An G and Schick M 1988 *J. Phys. A: Math. Gen.* **21** L213
- [19] Zhu L and DePristo A E 1995 *J. Chem. Phys.* **102** 5342  
Zhu L and DePristo A E 1997 *J. Catal.* to be published
- [20] DePristo A E 1995 private communication